This Accepted Manuscript has not been copyedited and formatted. The final version may differ from this version.

eNeuro

Research Article: New Research | Cognition and Behavior

Mesocortical Dopamine Phenotypes in Mice Lacking the Sonic Hedgehog Receptor Cdon

Dopamine Phenotypes of Cdon−/− Mice

Michael Verwey[1,2], Alanna Grant[1], Nicholas Meti[2], Lauren Adye-White[1], Angelica Torres-Berrío[1], Veronique Rioux[6,7], Martin Lévesque[6,7], Frederic Charron[2,3,4,5,*] and Cecilia Flores[1,*]

[1]*Department of Psychiatry, Douglas Mental Health University Institute, McGill University, Montreal, QC H4H 1R3, Canada*

[2]*Molecular Biology of Neural Development, Institut de Recherches Cliniques de Montréal, Montreal, QC H2W 1R7, Canada*

[3]*Department of Medicine, University of Montreal, Montreal, QC H3T 1J4, Canada*

[4]*Department of Anatomy and Cell Biology, Department of Biology, Division of Experimental Medicine, McGill University, Montreal, QC H3A 0G4, Canada*

[5]*Program in Neuroengineering, McGill University, Montreal, QC H3A 0G4, Canada*

[6]*Department of Psychiatry and Neurosciences, Faculty of Medicine, Université Laval, Québec, QC, Canada*

[7]*Centre de Recherche Université Laval-Robert-Giffard, Université Laval, Québec, QC G1J 2G3, Canada*

DOI: 10.1523/ENEURO.0009-16.2016

Received: 14 January 2016

Revised: 22 June 2016

Accepted: 22 June 2016

Published: 29 June 2016

Author contributions: M.V., A.G., M.L., F.C., and C.F. designed research; M.V., A.G., N.M., L.A.-W., A.T.-B., and V.R. performed research; M.V., A.G., N.M., L.A.-W., A.T.-B., and V.R. analyzed data; M.V., F.C., and C.F. wrote the paper.

Funding: Canadian HIV Trials Network, Canadian Institutes of Health Research (Réseau canadien pour les essais VIH des IRSC)
501100002879

Funding: Fonds de Recherche du Québec - Santé (Fonds de la recherche en sante du Quebec)
501100000156

Funding: Natural Science and Engineering Research Council

Funding: Canada Foundation for Innovation

The authors declare no competing financial interests.

This work was supported by grants from the Canadian Institutes of Health Research to F.C. and C.F., the Fonds de Recherche du Québec-Santé (FRQS) to F.C. and C.F., the Canada Foundation for Innovation to F.C. and C.F., and the Natural Science and Engineering Research Council of Canada (NSERC) to M.L. and C.F. M.V. is the recipient of FRQS and NSERC postdoctoral research fellowships. M.L. and C.F. are FRQS Research Scholars. F.C. holds the Canada Research Chair in Developmental Neurobiology.

*F.C. and C.F. contributed equally to this work.

Correspondence should be addressed to either of the following: Frederic Charron, 2Molecular Biology of Neural Development, Institut de Recherches Cliniques de Montréal (IRCM), 110 Pine Avenue West, Montreal, QC H2W 1R7, Canada, E-mail: frederic.charron@ircm.qc.ca; or Cecilia Flores, Department of Psychiatry, Douglas Mental Health University Institute, McGill University, 6875 LaSalle Boulevard, Montreal, QC H4H 1R3, Canada, E-mail: cecilia.flores@mcgill.ca.

Cite as: eNeuro 2016; 10.1523/ENEURO.0009-16.2016

Alerts: Sign up at eneuro.org/alerts to receive customized email alerts when the fully formatted version of this article is published.

Accepted manuscripts are peer-reviewed but have not been through the copyediting, formatting, or proofreading process.

This is an open-access article distributed under the terms of the Creative Commons Attribution 4.0 International (http://creativecommons.org/licenses/by/4.0), which permits unrestricted use, distribution and reproduction in any medium provided that the original work is properly attributed.

Copyright © 2016 Society for Neuroscience

eNeuro Accepted Manuscript

eNeuro Accepted Manuscript

Manuscript Title Page:

1. **Manuscript Title:** Mesocortical Dopamine Phenotypes in Mice Lacking the Sonic Hedgehog Receptor Cdon
2. **Abbreviated Title:** Dopamine phenotypes of *Cdon*$^{-/-}$ mice
3. **List of all Author Names and Affiliations in order as they would appear in the published article:**

Verwey M.[1,2], Grant A.[1], Meti N.[2], Adye-White L.[1], Torres-Berrío A.[1], Rioux V.[6,7], Lévesque M.[6,7], Charron F.[2,3,4,5,*], Flores C.[1,*]

1. Department of Psychiatry, Douglas Mental Health University Institute, McGill University, 6875 LaSalle Boulevard, Montreal, QC, H4H 1R3, Canada
2. Molecular Biology of Neural Development, Institut de Recherches Cliniques de Montréal (IRCM), 110 Pine Avenue West, Montreal, QC, H2W 1R7, Canada
3. Department of Medicine, University of Montreal, Montreal, QC, H3T 1J4, Canada
4. Department of Anatomy and Cell Biology, Department of Biology, Division of Experimental Medicine, McGill University, Montreal, QC, H3A 0G4, Canada
5. Program in Neuroengineering, McGill University, Montreal, QC, H3A 0G4, Canada
6. Department of Psychiatry and Neurosciences, Faculty of Medicine, Université Laval, Québec, QC, Canada
7. Centre de Recherche Université Laval-Robert-Giffard, Université Laval, 2601 Chemin de la Canardière, Quebec, QC, G1J 2G3, Canada

*Equal contribution

eNeuro Accepted Manuscript

4. **Author Contributions: Verwey, M.** (Designed research, Performed research, Analyzed data, Wrote the manuscript), **Grant A.** (Designed research, Performed research, Analyzed data, Proofed final paper), **Meti N.** (Designed research, Performed research, Analyzed data), **Adye-White L.** (Performed research, Analyzed data), **Torres-Berrío A.** (Performed research, Analyzed data), **Rioux V.** (Performed research, Analyzed data), **Lévesque M.** (Designed research, Proofed final paper), **Charron F.** (Designed research, Wrote and edited the manuscript), **Flores C.** (Designed research, Wrote and edited the manuscript)
5. **Correspondence should be addressed to:**

Corresponding authors: frederic.charron@ircm.qc.ca and cecilia.flores@mcgill.ca

Submitting author: michael.verwey@gmail.com

6. **Number of Figures: 7**
7. **Number of Tables: 1**
8. **Number of Multimedia: 0**
9. **Number of words for Abstract: 251**
10. **Number of words for significance statement: 107**
11. **Number of words for Introduction: 655**
12. **Number of words for discussion: 1845**
13. **Acknowledgements:**

We thank Colleen Manitt, Doris Zhu, Heshmat Rajabi, Sandra Yogendran, Jimmy Peng, Steves Morin, Dominique Nouel, Jessica Barthe, and Lukas Tamayo-Orrego for help and advice. This work was supported by grants from the Canadian Institutes of Health

eNeuro Accepted Manuscript

Research (CIHR) to CF and FC, the Fonds de Recherche du Québec-Santé (FRQS) to CF and FC, the Canada Foundation for Innovation (CFI) to CF and FC, and the Natural Science and Engineering Research Council of Canada (NSERC) to CF and ML. MV is recipient of FRQS and NSERC postdoctoral research fellowships. CF and ML are FRSQ Research Scholars. FC holds the Canada Research Chair in Developmental Neurobiology.

14. **Conflict of interest:** Authors report no conflict of interest

15. **Funding Sources:** Canadian Institutes of Health Research, Fonds de Recherche du Québec-Santé, Canada Foundation for Innovation, Natural Science and Engineering Research Council of Canada, Canada Research Chair

eNeuro Accepted Manuscript

ABSTRACT

Motivated behaviors and many psychopathologies typically involve changes in dopamine release from the projections of the ventral tegmental area (VTA) and/or the substantia nigra pars compacta (SNc). The morphogen Sonic Hedgehog (Shh) specifies fates of midbrain dopamine neurons, but VTA-specific effects of Shh signaling are also being uncovered. In this study we assessed the role of the Shh receptor Cdon in the development of VTA and SNc dopamine neurons. We find that Cdon is expressed in the proliferating progenitor zone of the embryonic ventral midbrain and that the number of proliferating cells in this region is increased in mouse *Cdon*$^{-/-}$ embryos. Consistent with a role of Shh in the regulation of neuronal proliferation in this region, we find that the number of TH-positive neurons is increased in the VTA of *Cdon*$^{-/-}$ mice at birth and that this effect endures into adulthood. In contrast, the number of TH-positive neurons in the SNc is not altered in *Cdon*$^{-/-}$ mice at either age. Moreover, adult *Cdon*$^{-/-}$ mice have a greater number of medial prefrontal cortex (mPFC) dopamine presynaptic sites, and increased baseline concentrations of dopamine and dopamine metabolites selectively in this region. Finally, consistent with increased dopamine function in the mPFC, we find that adult *Cdon*$^{-/-}$ mice fail to exhibit behavioral plasticity upon repeated amphetamine treatment. Based on these data, we suggest that Cdon plays an important role encoding the diversity of dopamine neurons in the midbrain, influencing both the development of the mesocortical dopamine pathway and behavioral outputs that involve this neural circuitry.

eNeuro Accepted Manuscript

87 **SIGNIFICANCE STATEMENT**

88 Sonic hedgehog signaling is involved in the specification and development of dopamine neurons
89 in the ventral midbrain. Here we demonstrate that the Shh receptor, Cdon, plays a role in the
90 development of dopamine neurons in the ventral tegmental area. Moreover, this effect of
91 Cdon is selective to the dopamine neurons that project to the medial prefrontal cortex. Adult
92 mice that lack Cdon also fail to show amphetamine-induced behavioral plasticity. Our findings
93 show that the Cdon receptor is important in encoding the diversity of dopamine neurons in the
94 midbrain, influencing both the development of the mesocortical dopamine pathway as well as
95 behavioral outputs that involve this neural circuitry.

96

eNeuro Accepted Manuscript

INTRODUCTION

Midbrain dopamine neurons are involved in diverse behavioral and psychological processes and alterations in their development can have implications that range from motor deficits to psychopathology (Bjorklund and Dunnett, 2007; Blesa and Przedborski, 2014; Volkow and Morales, 2015). Dopamine neurons in the ventral tegmental area (VTA) and substantia nigra pars compacta (SNc) share basic neurochemical similarities, but increasing evidence shows that they are heterogeneous and that their physiological properties vary in a target-dependent manner (Roeper, 2013). Likewise, developmental mechanisms that define the segregation of VTA and SNc dopamine neurons, and the unique cortical and striatal projections that they make, have also begun to emerge (Van den Heuvel and Pasterkamp, 2008; Anderegg et al., 2015; Bissonette and Roesch, 2015).

One example is the Sonic hedgehog (Shh) signaling pathway, which is involved in the specification of dopamine cell fate (Hynes et al., 1995; Wang et al., 1995; Wallen and Perlmann, 2003) and acts as a chemoattractant that promotes the rostral projections of these neurons (Hammond et al., 2009). In order to activate the Shh pathway, Shh binds to Patched1 (Ptch1), which leads to Smoothened (Smo) disinhibition and the activation of Gli transcription factors. Shh signaling acts in two phases during the specification of dopaminergic neurons: during the first phase, notochord-derived Shh initiates the specification of the ventral midbrain, including the progenitors of dopamine neurons. During the second phase, Shh is expressed by dopamine neuron progenitors themselves, and the duration of Shh expression contributes to their fate decisions and their segregation between the VTA and SNc (Blaess et al., 2011; Hayes et al., 2011; Hayes et al., 2013). Therefore, the fate decisions of dopamine progenitors and the

eNeuro Accepted Manuscript

numbers of dopamine cells in the VTA and/or SNc are differentially influenced by Shh signaling, depending on how and at what developmental time the Shh signaling pathways is manipulated (Blaess et al., 2011; Hayes et al., 2011; Hayes et al., 2013; Kabanova et al., 2015). As a result, variations in Shh signaling, at selective developmental times, must influence behaviors in adulthood that depend on mesocorticolimbic and/or nigrostriatal dopamine pathways. Such variations in Shh signaling might therefore be involved in distinct psychopathologies.

Cell adhesion molecule-related/down-regulated by oncogenes (Cdon) is a Ptch1 co-receptor that binds Shh (Okada et al., 2006) and modulates pathway activity (Okada et al., 2006; Allen et al., 2011; Yam and Charron, 2013). The role of Cdon in segregating dopamine neurons between the VTA and SNc, and its potential impacts on behavior, have never been explored. Here we show that Cdon is expressed in the embryonic ventral midbrain dopaminergic progenitors. Based on this finding we hypothesized that Cdon could mediate some of the general, and possibly region-specific (i.e. VTA versus SNc) effects of Shh on the development of the dopamine system and, in turn, influence dopamine-mediated behaviors in adulthood. To this end, we compared wildtype (WT) and *Cdon*$^{-/-}$ embryos at e12.5, and identified a potential role for Cdon in the regulation of proliferation in the midbrain dopaminergic progenitors. Consistent with a putative increase in the proliferation of dopamine progenitors in *Cdon*$^{-/-}$ mice, we observed an increase in the number of dopamine neurons in *Cdon*$^{-/-}$ mice immediately after birth and in adult life. Importantly, this increase was specifically observed in the VTA. Next, we examined dopamine concentrations in forebrain regions that receive dopamine projections from the VTA or the SNc and found increased levels of dopamine and dopamine metabolites in the medial prefrontal cortex (mPFC), but not in the nucleus

eNeuro Accepted Manuscript

accumbens (NAcc) and dorsal striatum (DS), of adult *Cdon*$^{-/-}$ mice. Furthermore, we found that adult *Cdon*$^{-/-}$ mice have increased number of mPFC dopamine presynaptic sites. To determine potential behavioral consequences of these neuroanatomical and neurochemical changes, we evaluated amphetamine-induced behavioral plasticity in adult *Cdon*$^{-/-}$ mice and found important deficits. These findings show that Cdon is important in the development of VTA dopamine neurons, particularly those projecting to the mPFC, and in turn influences adult behaviors that are dependent on these pathways.

eNeuro Accepted Manuscript

METHOD

Animal housing and breeding – All animal housing, experiments, and procedures were approved by the Animal Care Committee at the Douglas Mental Health University Institute, McGill University (Montreal, Canada), and at the Institut de Recherches Cliniques de Montréal (IRCM), and were all in accordance with the guidelines set out by the Canadian Council of Animal Care (http://www.ccac.ca). *Cdon*$^{-/-}$ mice (Okada et al., 2006) were generated by a gene trap vector that targeted the transmembrane domain of Cdon (Friedel et al., 2005), and were backcrossed with C57BL/6 mice for at least 10 generations. Experimental *Cdon*$^{-/-}$ mice were generated by crossing *Cdon*$^{+/-}$ breeders. Male and female offspring were pooled for embryonic and postnatal day (PND) 0 studies, as well as in the quantification of TH-positive varicosities in the mPFC. All other experiments used only male mice.

Immunohistochemistry and Stereological Analyses

Tissue Preparation and Sectioning – Embryos and PND 0 pups were dissected, post-fixed in a 4% paraformaldehyde solution (24h, 4°C), cryoprotected in a sucrose solution (24h, 15% sucrose, 4°C), then snap frozen in optimal cutting temperature medium (Tissue-Tek, Cedarlane, Burlington, Ontario) and stored at -80°C until slicing. Embryos (14µm sections) and PND 0 (35µm sections) were sliced on a cryostat (Leica CM3050S, Concord, Ontario), sections were collected on charged superfrost slides (Fisherbrand, Ottawa, Ontario), and stored at -80°C until use. Adult male mice (postnatal day 75 ±15) were deeply anesthetized with sodium pentobarbital (>75mg/kg, intraperitoneal; i.p.), perfused transcardially with ~50ml of 0.9% saline followed by ~50ml of 4% paraformaldehyde. Brains were dissected and post-fixed

eNeuro Accepted Manuscript

overnight (4°C) and sliced on a Vibratome (35µm sections, Leica, Concord, Ontario). Serial coronal sections were stored free-floating in Watson's cryoprotectant at -20°C until processing (Watson et al., 1986).

Immunohistochemistry – Immunohistochemistry and immunofluorescent staining was performed (Okada et al., 2006; Manitt et al., 2010; Manitt et al., 2011; Mille et al., 2014) with anti-tyrosine hydroxylase (TH) mouse (1:1000, MAB318, Millipore Bioscience Research Reagents, Etobicoke, Ontario, Canada), anti-TH rabbit (1:1000, MAB152, Millipore Bioscience Research Reagents, Etobicoke, Ontario, Canada), anti-Ki67 mouse (1:250, #550609, BD Biosciences, Mississauga, ON), anti-Cdon Goat (1:500, AF2429, R&D Systems), and anti-βGal Rabbit (1:1000, #0855976, MP Biologicals, Solon, OH) antibodies. Antigen retrieval was used prior to all embryonic labeling, and Alexa-488, Alexa-555, or Alexa-643 conjugated secondary antibodies (Molecular Probes, Eugene, OR, USA) were used for immunofluorescence. For PND 0 and adult stereology experiments that quantified TH-positive cells in the VTA and SN, a 3% hydrogen peroxide pre-treatment was used to inactivate endogenous peroxidases, and a 3,3'-Diaminobenzidine kit was used according to manufacturer instructions (PK-4000 ABC kit, SK-4100 DAB kit, Vector Laboratories). For stereological quantification of TH-positive varicosities in the mPFC, TH was visualized with an Alexa-555 conjugated secondary antibody.

Microscopy and Analysis – Serial coronal sections of embryos and adult brains were examined with Leica DM4000 and DM6000 microscopes with an Orca ER CCD camera (Hamamatsu) using Volocity (PerkinElmer, Waltham, MA, USA) or Stereoinvestigator (MBF Bioscience, Williston, VT,

eNeuro Accepted Manuscript

193 USA) software. In order to avoid including mice with signs of holoprosencephaly (HPE), we
194 inspected for HPE on the live/intact mouse or embryo and carried out a careful and systematic
195 morphological analysis under the microscope. Specifically, all embryos and mice were
196 inspected for any signs of cebocephaly and incomplete forebrain clefting (Zhang et al., 2006). At
197 PND0, we observed a single instance of malformed olfactory bulbs, which is another sign of HPE
198 and led to the exclusion of this mouse (Zhang et al., 2006). Finally, across all ages, we examined
199 carefully for enlarged or malformed ventricles. We also verified that mice did not show tooth
200 malformations, which is another symptom of Cdon-associated HPE (Cole and Krauss, 2003), and
201 weighed mice regularly to identify possible difficulties eating. All the adult *Cdon*$^{-/-}$ mice included
202 in the study had similar weights to the WT littermates.

203 Embryonic TH and Ki67 immunoreactivity was counted manually with ImageJ software,
204 and averaged for at least 2 sections/level/embryo, and analyzed by two-way $ANOVA_{GenotypeXLevel}$.
205 Stereology was performed to quantify the number of TH-positive cell bodies in the VTA and
206 SNc, and the number of TH-positive varicosities in the mPFC (Manitt et al., 2013; Daubaras et
207 al., 2014). Briefly, the number of TH-positive cells were counted in the VTA and SNc of *Cdon*$^{-/-}$
208 mice and WT littermate controls at PND 0 and PND 75±15 with a stereological fractionator
209 sampling design (West et al., 1991), and Stereoinvestigator software (MBF Bioscience, Williston,
210 VT). The VTA- and SNc-containing sections ranged from Plates 54-57 of the mouse brain atlas
211 (Franklin and Paxinos, 2007). The counting frame (75µm x 75µm) and grid size (150µm x
212 150µm) were chosen manually. Counting was carried out using every other brain section. A
213 guard zone of 5µm at the top and bottom of the section was used, and the coefficient of error
214 was below 0.1 in all animals studied, and the experimenter was blind to experimental groups.

eNeuro Accepted Manuscript

To obtain a measure of the presynaptic density of dopamine synapses in the pregenual mPFC, TH-positive varicosities were quantified in this structure. TH-positive varicosities are sites of putative synapses with a dendritic spine or shaft (Seguela et al., 1988), and are where neurotransmitter synthesis, release, and reuptake generally occur (Benes et al., 1996). Consistent with previous neuroanatomical studies (Manitt et al., 2011; Reynolds et al., 2015), and because of the lateralization of the dopamine system, we only obtained counts from the right hemisphere. Using stereoinvestigator software (MicroBrightField), we made stereological quantifications of the volume and of number of TH-positive varicosities in the cingulate (Cg), prelimbic (PL), and infralimbic (IL) subregions of the mPFC. These subregions were delineated according to plates 14–18 of the mouse brain atlas (Paxinos and Franklin, 2008) and contours of the dense TH-positive innervation within each subregion was traced at 5x magnification using a Leica DM4000 microscope. An unbiased counting frame (25µm x 25µm) was superimposed on each contour, and counts were made at regular predetermined intervals (175µm x 175µm). All counting of varicosities was performed at 100x magnification on 6 of the 12 sections contained within the rostrocaudal borders of our region of interest (1:2 series). Guard zones (4µm) and an optical dissector (10µm) were used. We used the Cavalieri method in Stereoinvestigator (MicroBrightField) to assess the volume of TH-positive fiber innervation (μm^3), and the optical fractionator probe was then used to count TH-positive varicosities. The gunderson coefficient of error was below 0.15 for all regions of interest in all sampled brains.

Analysis of dopamine and dopamine metabolite concentrations in rostral targets of midbrain dopamine neurons

eNeuro Accepted Manuscript

Tissue preparation – As described previously (Grant et al., 2009; Grant et al., 2014), mice were decapitated, brains were rapidly dissected and snap frozen in 2-methylbutane (Fisher Scientific, Hampton, NH, USA) on dry ice. Brains were then sliced on a cryostat and 0.5mm punches (Cat#18035-50, Fine Science Tools, North Vancouver, British Columbia) were taken bilaterally to dissect the pregenual mPFC (pooling Cg, PL, and IL subregions), NAcc (including both shell and core), and a 1.0mm punch was taken DS (dorsolateral portion), then all samples were frozen at -80°C until use.

High-Performance Liquid Chromatography (HPLC) – Levels of dopamine, 3,4-dihydroxyphenylacetic acid (DOPAC) and homovanillic acid (HVA) in the DS, NAcc, and mPFC were assessed using HPLC (Grant et al., 2007). Briefly, brain punches from each area were homogenized in a 0.1M phosphate buffer, centrifuged, the supernatant was then removed and filtered for HPLC testing, and the pellet was re-suspended for quantification of the protein content (Bicinchoninic acid kit, Thermo Scientific, Catalog # P123225, Waltham, MA, USA). The HPLC assay for dopamine, DOPAC, and HVA was performed with an EZChrom chromatography system (Scientific Software Inc., San Ramon, CA, USA). Dopamine and metabolites were detected and quantified with a Coulochem III detector and concentrations were calculated from peak height comparisons with known amounts of injected pure standards (Sigma). Significance levels used to evaluate statistical differences were adjusted using the Holm-Bonferroni sequentially rejective procedure (Holm, 1979).

Behavioral testing

eNeuro Accepted Manuscript

Locomotor activity testing – As described previously (Grant et al., 2009; Yetnikoff et al., 2010), locomotor activity was measured by an infrared system that monitors total horizontal distance travelled within a defined period of time (AccuScan Instruments, Columbus, OH, USA). On day 1, mice were habituated to the locomotor chambers for 15-min. On day 2, following a 15-min habituation period, mice were habituated to the injection procedure with an i.p. injection of saline, and locomotor activity was recorded for 30-min. On day 3, after habituation, mice were given 2.5mg/kg of d-amphetamine (i.p.) and locomotor activity was monitored for another 90-min. Next, all mice were given 4mg/kg d-amphetamine every other day, for a total of 5 additional injections, delivered on days 5, 7, 9, 11, and 13. Finally, on day 21, after 8 days of drug abstinence in their home cages, mice were tested again with 2.5mg/kg d-amphetamine (A diagram illustrating this schedule can be seen in Figure 7D). Differences between the locomotor activity induced by the first dose of amphetamine (day 3) and the last dose of amphetamine (day 21) represent a form of behavioral plasticity known as locomotor sensitization (Stewart and Badiani, 1993; Pierce and Kalivas, 1997).

Pre-pulse inhibition (PPI) – As described previously (Grant et al., 2007), PPI was assessed using sound attenuated startle chambers (SR-LAB, San Diego Instruments, San Diego, USA) containing a clear restraining tube that housed the animal throughout the testing session and background white noise (70dB) was delivered continuously. Prior to each session, all chambers were calibrated to ensure consistent sensitivity and stable sound levels between testing boxes. A 120dB pulse induced a startle response in mice, which was recorded by computer, and was an average of 65 readings taken at 1ms intervals after the startle pulse. Each pre-pulse was

eNeuro Accepted Manuscript

delivered 100ms before the acoustic startle, and lasted 20ms. Within each session there were a total of 54 trials in a pseudo-random order, which included 12 startle trials with no pre-pulse, 6 trials with pre-pulses at each volume (3, 5, 7, 10, 15, and 20 dB, above the 70dB background noise), and 6 null trials where no acoustic startle was presented. The degree of PPI was then calculated as a percentage for each pre-pulse intensity: PPI% = 1-(mean pre-pulse – mean null)/(mean startle – mean null)*100.

Statistical Analyses

All Student's t-tests, analyses of variance, and Bonferroni post-hoc tests were performed using Prism 5 (GraphPad Software Inc., La Jolla, CA, USA). For each Figure and statistical test, F and t values are reported in Table 1. Specifically, in Figures 2C and 2E Student's t-tests were used, and in Figures 2D and 2F 2-way $ANOVA_{GenotypeXLevel}$ were used. In Figure 3, stereological means were compared within each brain area by Student's t-test. In Figure 4, planned comparisons were made using the Holm-Bonferroni sequentially rejective procedure (Holm, 1979). In Figure 5, a 2-way $ANOVA_{GenotypeXRegion}$ was used. In Figure 6A, 6B, and 6C, two-way $ANOVA_{GenotypeXTime}$ were used to compare groups over the test, and in Figure 6E and 6F, two-way $ANOVA_{GenotypeXTime}$ were used with Bonferroni post-hoc comparisons. In Figure 7, a 2-way $ANOVA_{GenotypeXppvolume}$ was used

.

eNeuro Accepted Manuscript

RESULTS

Cdon is expressed in proliferating midbrain dopamine progenitor cells at E12.5

We assessed whether Cdon is expressed in the embryonic ventral midbrain. This was done using two complementary approaches in the ventral midbrain of e12.5 embryos (Figure 1A). First, we used mice in which a gene encoding β-Galactosidase (β-Gal) was inserted in the *Cdon* gene by homologous recombination (Okada et al., 2006) and assessed β-Gal expression by immunofluorescence in *Cdon*$^{+/-}$ embryos. Periventricular and ventral β-Gal labeling was observed in a zone where progenitors proliferate and differentiate into dopamine neurons, as shown in Figure 1B (top panel). As a negative control, no β-Gal labeling was observed in *Cdon*$^{+/+}$ embryos under the same conditions (Figure 1B, bottom panel). As a second approach, immunolabeling against the Cdon protein showed a very similar Cdon localization in the ventral midbrain of WT embryos (Figure 1C, top and middle panels), confirming the results obtained using the β-Gal reporter. We next analyzed Cdon expression (using the β-Gal reporter) in the context of proliferating (Ki67), immature (Nuclear receptor related *1,* Nurr1), and mature dopamine neurons expressing tyrosine hydroxylase (TH) in the ventral midbrain. We found that at e12.5, Cdon(β-Gal) expression was dorsal to, and did not overlap with, the TH-positive zone (Figure 1D, top panel). Based on labeling in adjacent sections, there was a small overlap with immature dopamine neurons expressing Nurr1 but not TH (Figure 1D, middle panel). However, Cdon(β-Gal) expression was strongest in the proliferative, Ki67-positive, progenitor zone (Figure 1D, bottom panel). Therefore, at e12.5, Cdon is mostly expressed in the proliferating midbrain dopamine progenitors.

eNeuro Accepted Manuscript

Increased number of proliferating cells in the ventral midbrain of *Cdon*$^{-/-}$ embryos at e12.5

In order to assess the role of Cdon in the development of dopamine neurons, *Cdon*$^{-/-}$ and WT littermates were stained for Ki67 and TH at e12.5. Representative images of immunofluorescence are shown in Figure 2A, which are coronal sections from the ventral midbrain (Figure 2B). *Cdon*$^{-/-}$ embryos exhibited a significant increase in the number of Ki67-positive cells on the ventricular border in comparison to WT littermates (Figure 2C; Unpaired t-test, p=0.0069, Table 1-a). Moreover, this effect was observed across the anterior-posterior axis (Figure 2D; $ANOVA_{Genotype}$, p=0.0003, Table 1-b). This increase in Ki67 indicates that there is an increased level of proliferation of neural progenitors in the ventral midbrain of *Cdon*$^{-/-}$ embryos. In contrast, at the same embryonic stage, the number of TH-positive neurons was similar between genotypes (Figure 2E; unpaired t-test, Table 1-c). This was also true when individual levels of the anterior-posterior axis were investigated (Figure 2F, $ANOVA_{GenotypeXLevel}$, Table 1-d). These results indicate that inactivation of *Cdon* causes an increase in the number of proliferating progenitors, but that e12.5 could be still be too early to observe a change in the number of cells expressing TH.

Postnatal increase in the number of TH-positive neurons in the VTA of *Cdon*$^{-/-}$ mice

We next assessed whether this increase in progenitor proliferation leads to an increase in numbers of dopamine neurons later in brain development and in adulthood. Stereological counts of TH-positive neurons in the VTA and SNc at postnatal day (PND) 0 revealed a significant increase in the number of TH-positive cells in the VTA of *Cdon*$^{-/-}$ mice compared to WT littermates (Figure 3A, left graph; Student's t-test, p=0.01, Table 1-e). In contrast, the

eNeuro Accepted Manuscript

number of TH-positive cells in the SNc is not significantly changed between genotypes (Figure 3A, right graph; Student's t-test, Table 1-e). Interestingly, the same pattern is observed in adult mice, where there are more TH-positive neurons in the VTA of adult *Cdon*$^{-/-}$ mice in comparison to WT littermates (Figure 3B, left graph; Student's t-test, p=0.006; Table 1-f, and Figure 3C), but there are no genotype differences in TH-positive cell counts in the SNc (Figure 3B, right graph, Table 1-f). These data show that there is an early, enduring, increase in the number of TH-positive neurons in *Cdon*$^{-/-}$ mice compared to WT littermates. Interestingly, this increase is selective to the medial portion (i.e. VTA region) of the midbrain dopamine somatodendritic region.

Selective increase in dopamine levels in the PFC of adult *Cdon*$^{-/-}$ mice

To examine whether the increase in the number of TH-positive neurons in the VTA is associated with differential content of dopamine and the dopamine metabolites dihydroxyphenylacetic acid (DOPAC) and homovanillic acid (HVA) in forebrain terminal regions, we conducted high-performance liquid chromatography (HPLC) on tissue samples of VTA and SNc targets: mPFC, NAcc, and DS (illustrations shown in Figure 4A). As shown in Figure 4B (top panel), in the mPFC the levels of dopamine and DOPAC of *Cdon*$^{-/-}$ mice are significantly elevated compared to WT littermates (Student's t-test with Holm-Bonferroni correction, Dopamine p=0.03, DOPAC p=0.019, Table 1-g). In contrast, there were no differences between genotypes in concentrations of dopamine, DOPAC, and HVA in the NAcc (Figure 4B, middle panel, Table 1-g) or DS (Figure 4B, bottom panel, Table 1-g). These findings suggest that the increase in the

eNeuro Accepted Manuscript

number of TH-positive cells in the VTA of *Cdon*$^{-/-}$ mice is specific to VTA dopamine neurons that project to the mPFC.

Increased number of TH-positive varicosities in the mPFC of *Cdon*$^{-/-}$ mice

We then performed stereological quantifications of dopamine varicosities in the Cg, PL, IL sub-regions (Figure 5A) of the pregenual mPFC. We found a significant increase in the total number of dopamine varicosities (i.e. dopamine presynaptic sites) in the Cg, PL, and IL subregions of the mPFC of *Cdon*$^{-/-}$ mice in comparison to controls (Figure 5B, $ANOVA_{Genotype}$, p=0.0079, Table 1-h). To determine whether this increase in the total number of dopamine presynaptic sites results from enhanced expanse of the dopamine innervation to the mPFC, we quantified the volume of the dopamine input to each subregion using the Cavalieri method (Manitt et al., 2011; Reynolds et al., 2015). There were no differences in dopamine input volume between genotypes in any of the subregions examined, indicating that dopamine axons in *Cdon*$^{-/-}$ mice are not extending to other mPFC layers (Figure 5C, $ANOVA_{Genotype}$, Table 1-i). This led to a significant increase in the density of dopamine varicosities in all three subregions (Figure 5D, $ANOVA_{Genotype}$, p=0.0073, Table 1-j), which could be seen at high magnification (Figure 5E).

Locomotor activity of *Cdon*$^{-/-}$ mice reveals an attenuation of behavioral plasticity in adulthood

To examine possible consequences of the neuroanatomical changes that we observed in the VTA and mPFC of *Cdon*$^{-/-}$ mice, we evaluated the locomotor responses of adult *Cdon*$^{-/-}$ and WT mice. Both genotypes exhibited similar levels of locomotor activity when placed in the novel locomotor testing environment (Figure 6A, Table 1-k) and in response to a saline injection

eNeuro Accepted Manuscript

(Figure 6B, Table 1-l). *Cdon*$^{-/-}$ and WT mice also responded identically to the first dose of d-amphetamine (2.5mg/kg; Figure 6C, Table 1-m). Thus, *Cdon*$^{-/-}$ and WT littermates respond with similar amounts of locomotor activity in response to novelty and to single exposure to a stressor (e.g. saline injection) or a stimulant drug of abuse (e.g. amphetamine).

The amount of locomotor activity typically increases with repeated drug experience, a phenomenon known as sensitization. In order to test locomotor sensitization, mice were given 5 doses of 4mg/kg d-amphetamine every other day (over the next 2.5 weeks) and then left undisturbed in their home cage for 8 days (schedule depicted in Figure 6D). Mice were then tested at the same 2.5mg/kg dose that was used on the first trial, ~3 weeks previously. WT mice exhibited robust locomotor sensitization, and when pre- and post- sensitization levels were compared, the amount of locomotor activity nearly doubled (Figure 6E, Within-subjects Bonferroni Post hoc on WT, p=0.0018, Table 1-n). In contrast, no change in the amount of locomotor activity was observed in the *Cdon*$^{-/-}$ mice when pre- and post- sensitization levels were compared (Figure 6E). Of note, drug-induced stereotypy (repetitive behavior) was also increased in WT mice over time (Figure 6F, Within-subjects Bonferroni Post hoc on WT, p=0.027, Table 1-o), but did not change significantly in *Cdon*$^{-/-}$ mice (Figure 6F). These data demonstrate that while baseline locomotor responses to stress and to an initial dose of amphetamine were indistinguishable between *Cdon*$^{-/-}$ and WT mice, amphetamine-induced behavioral plasticity is attenuated in *Cdon*$^{-/-}$ mice.

Attenuated sensorimotor gating function in adult *Cdon*$^{-/-}$ mice

eNeuro Accepted Manuscript

To further examine behavioral consequences of the neuroanatomical changes that we observed in *Cdon*$^{-/-}$ mice, we next tested sensorimotor gating function in adult mice, which can be modulated by alterations in mesocortical dopamine function (Swerdlow et al., 1990; Tenn et al., 2005; Grant et al., 2007). Rodents startle in response to loud noises and this reflex is typically reduced if an acoustic pre-pulse is given. The reduction in the startle magnitude is called pre-pulse inhibition (PPI) and louder pre-pulses typically produce greater PPI. As expected in WT mice, increasing the pre-pulse volume increases PPI (Figure 7, Main effect ppvolume, p=0.0001, Table 1-p). However, PPI was significantly reduced in *Cdon*$^{-/-}$ mice compared to WT littermates (Figure 7, Main effect of genotype, p=0.0006, Table 1-p).

eNeuro Accepted Manuscript

DISCUSSION

In this study we assessed the role of the Shh receptor Cdon in the development of VTA and SNc dopamine neurons. We found that Cdon is expressed in the proliferating progenitor zone of the embryonic ventral midbrain, and that the number of proliferating cells in this region is increased in *Cdon*$^{-/-}$ embryos. These findings indicate that Cdon is involved in the regulation of neuronal proliferation in progenitors of the ventral midbrain. Consistent with this idea, we found that the number of TH-positive neurons is increased in the VTA of *Cdon*$^{-/-}$ mice at birth and that this effect endures into adulthood. In contrast, the number of TH-positive neurons in the SNc is not significantly altered in *Cdon*$^{-/-}$ mice at either age. In accordance with an increase in the number of mesocortical VTA dopaminergic neurons, there is a greater number of dopamine presynaptic sites in the mPFC and corresponding increases in baseline concentrations of dopamine and dopamine metabolites selectively in this region in adult *Cdon*$^{-/-}$ mice. These data indicate that Cdon is selectively involved in the development of mesocortical dopamine neurons. Finally, we found that adult *Cdon*$^{-/-}$ mice fail to exhibit dopamine-dependent behavioral plasticity in response to repeated injections of amphetamine. Based on these data, we suggest that Cdon plays an important role in the encoding of diversity within the population of dopamine neurons of the midbrain, influencing both the development of the mesocortical dopamine pathway as well as behavioral outputs that involve this neural circuitry.

Cdon and dopaminergic neuron development

In the first phase of dopamine neuron specification, notochord-derived Shh initiates the specification of the ventral midbrain. Inactivation of Shh signaling at this phase leads to almost

eNeuro Accepted Manuscript

complete absence of dopaminergic neurons (Blaess et al., 2006). During the second phase, Shh is expressed by dopaminergic neuron progenitors and the duration of its expression contributes to their fate decisions into dopamine neurons and their segregation between VTA and SNc (Blaess et al., 2011; Hayes et al., 2011). Accordingly, inactivation of Shh signaling only after Shh is expressed within the dopamine progenitors (i.e. inactivation only during the second phase) leads to a VTA-specific increase in the number of dopamine cells, leaving the number of SNc dopamine cells unchanged (Hayes et al., 2013). Interestingly, this phenotype is very similar to what we observed in *Cdon*$^{-/-}$ mice, where we observed an increase in VTA dopaminergic neurons, but no change in SNc neurons. These results support the idea that the main role of Cdon is in the second phase of dopaminergic neuron induction. In agreement with this, we did not observe a difference in the number of TH-expressing neurons at e12.5, further indicating that Cdon plays a minor role, if any, in the first phase of dopaminergic neuron induction.

A previous study tested the importance of continued Shh expression in dopamine neurons in adult mice. Gonzalez-Reyes et al. (2012) used a Cre-Lox recombination strategy in order to selectively remove Shh from neurons that express the dopamine transporter. The dopamine transporter is a marker of mature dopamine neurons, and when Shh was removed from these neurons, premature degeneration was observed in the dopamine neurons of the SNc (Gonzalez-Reyes et al., 2012). Therefore, continued Shh expression is critical for the long-term maintenance of dopamine neurons in the SNc and nigrostriatal circuitry. Because we do not observe similar degeneration in the *Cdon*$^{-/-}$ mice, we propose that this Shh effect on adult SNc circuitry may not require Cdon.

eNeuro Accepted Manuscript

463 A previous report described a reduction in the number of TH-positive cells in e13.5
464 *Cdon*$^{-/-}$ embryos (Kwon et al., 2014). One possible reason for this discrepancy with our data is
465 the presence or absence of holoprosencephaly (HPE) in the *Cdon*$^{-/-}$ embryos analyzed. HPE is a
466 condition that results in inadequate formation of the neural midline and ventricle
467 malformation. Many studies have reported *Cdon*$^{-/-}$ mouse lines with as many as ~80% of
468 mutants showing HPE at birth, with virtually none surviving into adulthood (Cole and Krauss,
469 2003; Zhang et al., 2006; Bae et al., 2011; Zhang et al., 2011; Hong and Krauss, 2013). In
470 contrast, our *Cdon* mouse line exhibit a lower rate of HPE (~10-20%) and only mice that did not
471 show any obvious signs of HPE and that remained healthy into adulthood were included in our
472 study. This variability between studies is in part attributed to the fact that the expression of
473 HPE in *Cdon*$^{-/-}$ mice depends strongly on the genetic background and genetic modifiers of this
474 receptor (Cole and Krauss, 2003; Zhang et al., 2006; Bae et al., 2011). Importantly, HPE has
475 indeed been associated with decreased proliferation in primary neuronal cultures in *Cdon*
476 mutant mice (Zhang et al., 2006). Therefore, when present, HPE could potentially be acting in
477 opposition to the enhanced proliferation phenotype that we observed in our study.
478 The increased numbers of Ki67-positive cells that we observe at e12.5 coincides with the
479 second stage of Shh-signaling. At this stage in development, it would appear that Cdon
480 modulates the proliferation rate of dopamine neuron progenitors. Indeed, it has been shown
481 that once dopamine neuron progenitors begin to express Shh, the duration and timing of Shh
482 expression contributes to fate decisions made by these cells (Blaess et al., 2011; Hayes et al.,
483 2011). Therefore, mechanisms that alter the intensity or the duration of Shh-signaling and
484 expression are likely modified by removing the Shh receptor Cdon. This could result in

eNeuro Accepted Manuscript

485 increased numbers of proliferating dopamine neurons that go on to contribute mainly to the
486 mesocortical pool.

487 An increasing number of reports show that dopamine neurons in the VTA are a
488 heterogeneous population and that the neuroanatomical, electrophysiological, and
489 developmental properties of these neurons are dictated by the targets they innervate. It is
490 therefore possible that in the midbrain, only a subset of the medial portion of the ventral
491 midbrain dopamine neuron progenitors co-express Cdon and Shh, namely those dopamine
492 progenitors that are fated to innervate the mPFC. Increased numbers of mesocortical dopamine
493 neurons would presumably lead to increased dopamine input and dopamine concentrations to
494 the mPFC. Because the dopamine innervation to the mPFC is a protracted event, which extends
495 into early adulthood, we would also predict that these effects will only manifest fully in
496 adulthood. The fact that *Cdon*$^{-/-}$ mice exhibit greater number of presynaptic dopamine sites in
497 the mPFC without showing increases in the expanse that dopamine fibers occupy in this regions
498 indicates that Cdon plays a role in the proliferation of mesocortical dopamine neurons, but not
499 in their guidance towards forebrain targets.

500

501 **Cdon, mesocortical dopamine, and behavioral responses to drugs of abuse**

502 Locomotor responses to amphetamine depend mainly on drug-induced dopamine
503 release in the NAcc (Vezina et al., 1991; Vezina, 1993), which is influenced by dopamine
504 function in the mPFC (Bimpisidis et al., 2013). For example, mice that are haploinsufficient for
505 the Netrin-1 receptor *Dcc* exhibit increased baseline concentrations of dopamine and dopamine
506 metabolites in mPFC, which in turn causes blunted amphetamine-induced dopamine release in

eNeuro Accepted Manuscript

the NAcc (Flores et al., 2005; Pokinko et al., 2015). Interestingly, adult *Dcc* haploinsufficient mice also fail to show sensitization to the locomotor effects of amphetamine upon repeated exposure (Flores et al., 2005; Grant et al., 2007; Yetnikoff et al., 2010). Thus, it is likely that the behavioral changes observed in adult *Cdon*$^{-/-}$ mice could result from blunted responsiveness of NAcc-projecting dopamine neurons, associated with increased mPFC dopamine function (Bimpisidis et al., 2013).

The selective effects of Cdon on the mesocortical dopamine projections are particularly interesting in light of another recent study that also highlighted the sensitivity of this circuit to changes in Shh signaling (Kabanova et al., 2015). Gli2 is a transcription factor mediating many of the intracellular effects of Shh signaling in the brain (Vokes et al., 2007), and it is involved in the specification of dopamine neurons (Matise et al., 1998). Recently, Gli2 was conditionally removed from the cells of the ventral midbrain through En1-Cre-induced recombination (Kabanova et al., 2015). In these mice, dopamine levels were decreased in the mPFC, but not in the NAcc (Kabanova et al., 2015). Tracing experiments also demonstrated that the density of dopamine projection into the mPFC was reduced, whereas the density of dopamine fibers in the NAcc was not altered (Kabanova et al., 2015). While novel object learning was unimpaired in these mice, Kabanova et al. (2015) report increases in the amount of perseverative behavior during a five-choice serial reaction time task. This deficit in attention processing may be linked to the alterations in mPFC dopamine circuitry we observe in adult *Cdon*$^{-/-}$ mice (Moghaddam, 2002; Grace et al., 2007).

The relationship between increased dopamine concentrations in the mPFC and impaired PPI in *Cdon*$^{-/-}$ mice is surprising and at this point we cannot provide a conclusive mechanistic

eNeuro Accepted Manuscript

explanation of this finding. Deficits in baseline pre-pulse inhibition have been shown to result from *reduced* mesocortical dopamine function (Bubser and Koch, 1994; Swerdlow and Geyer, 1998; Kohl et al., 2013). Furthermore, because mesocortical dopamine function and responsiveness of mesolimbic dopamine neurons to stressors and drugs of abuse are inversely related (Jackson and Moghaddam, 2001; Ventura et al., 2004; Scornaiencki et al., 2009; Pokinko et al., 2015), it has been suggested that the role of mPFC dopamine on PPI is mediated by changes in ventral striatal dopamine function (Bubser and Koch, 1994; Koch and Bubser, 1994; Ellenbroek et al., 1996; Grant et al., 2007; Flores, 2011). However, there are no differences in nucleus accumbens dopamine concentrations between *Cdon*$^{-/-}$ and WT mice. It is possible that impaired sensorimotor gating function in *Cdon*$^{-/-}$ mice results from alterations in mPFC and/or nucleus accumbens dopamine release that could only be captured via *in vivo* microdialysis or voltammetry. Moreover, it is also possible that either insufficient or excessive extracellular dopamine concentration in the mPFC lead to deficits in PPI as it has been shown for the effects of mPFC dopamine function on cognitive processing (Floresco, 2013). Future studies will be aimed at addressing this issue directly using neurochemical and lesion approaches employed in previous studies (Jackson and Moghaddam, 2001; Ventura et al., 2004; Grant et al., 2007; Scornaiencki et al., 2009; Pokinko et al., 2015).

In conclusion, it is increasingly becoming clear that the diversity of midbrain dopamine neurons results from developmental processes that determine the heterogeneity of these cells, potentially long before this diversity can be accurately described (Anderegg et al., 2015). This diversity can be captured by comparing anatomical and functional properties of VTA and SNc dopamine neurons, but also by comparing electrophysiological properties of dopamine

eNeuro Accepted Manuscript

projections to cortical versus limbic targets (Lammel et al., 2008; Roeper, 2013), both of which are impossible to capture at early embryonic stages. In the current study, we demonstrate that the Shh receptor Cdon plays a specific role in the developmental organization and function of the mesocortical dopamine pathway. These changes also influence adult behavioral responses to drugs of abuse and sensorimotor gating. Our data therefore provide novel insights towards the diverse consequences of alterations in Shh signaling and describe changes in the VTA that have potential implications for psychopathologies such as schizophrenia (Meyer et al., 2008; Boyd et al., 2015) and attention deficit hyperactivity disorder (Heussler et al., 2002).

eNeuro Accepted Manuscript

REFERENCES

Allen BL, Song JY, Izzi L, Althaus IW, Kang JS, Charron F, Krauss RS, McMahon AP (2011) Overlapping roles and collective requirement for the coreceptors GAS1, CDO, and BOC in SHH pathway function. Dev Cell 20:775-787.

Anderegg A, Poulin JF, Awatramani R (2015) Molecular heterogeneity of midbrain dopaminergic neurons - Moving toward single cell resolution. FEBS Lett.

Bae GU, Domene S, Roessler E, Schachter K, Kang JS, Muenke M, Krauss RS (2011) Mutations in CDON, encoding a hedgehog receptor, result in holoprosencephaly and defective interactions with other hedgehog receptors. Am J Hum Genet 89:231-240.

Benes FM, Vincent SL, Molloy R, Khan Y (1996) Increased interaction of dopamine-immunoreactive varicosities with GABA neurons of rat medial prefrontal cortex occurs during the postweanling period. Synapse 23:237-245.

Bimpisidis Z, De Luca MA, Pisanu A, Di Chiara G (2013) Lesion of medial prefrontal dopamine terminals abolishes habituation of accumbens shell dopamine responsiveness to taste stimuli. Eur J Neurosci 37:613-622.

Bissonette GB, Roesch MR (2015) Development and function of the midbrain dopamine system: what we know and what we need to. Genes Brain Behav.

Bjorklund A, Dunnett SB (2007) Dopamine neuron systems in the brain: an update. Trends Neurosci 30:194-202.

Blaess S, Corrales JD, Joyner AL (2006) Sonic hedgehog regulates Gli activator and repressor functions with spatial and temporal precision in the mid/hindbrain region. Development 133:1799-1809.

Blaess S, Bodea GO, Kabanova A, Chanet S, Mugniery E, Derouiche A, Stephen D, Joyner AL (2011) Temporal-spatial changes in Sonic Hedgehog expression and signaling reveal different potentials

eNeuro Accepted Manuscript

583 of ventral mesencephalic progenitors to populate distinct ventral midbrain nuclei. Neural Dev
584 6:29.
585 Blesa J, Przedborski S (2014) Parkinson's disease: animal models and dopaminergic cell vulnerability.
586 Front Neuroanat 8:155.
587 Boyd PJ, Cunliffe VT, Roy S, Wood JD (2015) Sonic hedgehog functions upstream of disrupted-in-
588 schizophrenia 1 (disc1): implications for mental illness. Biol Open 4:1336-1343.
589 Bubser M, Koch M (1994) Prepulse inhibition of the acoustic startle response of rats is reduced by 6-
590 hydroxydopamine lesions of the medial prefrontal cortex. Psychopharmacology (Berl) 113:487-
591 492.
592 Cole F, Krauss RS (2003) Microform holoprosencephaly in mice that lack the Ig superfamily member
593 Cdon. Curr Biol 13:411-415.
594 Daubaras M, Dal Bo G, Flores C (2014) Target-dependent expression of the netrin-1 receptor, UNC5C, in
595 projection neurons of the ventral tegmental area. Neuroscience 260:36-46.
596 Ellenbroek BA, Budde S, Cools AR (1996) Prepulse inhibition and latent inhibition: the role of dopamine
597 in the medial prefrontal cortex. Neuroscience 75:535-542.
598 Flores C (2011) Role of netrin-1 in the organization and function of the mesocorticolimbic dopamine
599 system. J Psychiatry Neurosci 36:296-310.
600 Flores C, Manitt C, Rodaros D, Thompson KM, Rajabi H, Luk KC, Tritsch NX, Sadikot AF, Stewart J,
601 Kennedy TE (2005) Netrin receptor deficient mice exhibit functional reorganization of
602 dopaminergic systems and do not sensitize to amphetamine. Mol Psychiatry 10:606-612.
603 Floresco SB (2013) Prefrontal dopamine and behavioral flexibility: shifting from an "inverted-U" toward
604 a family of functions. Front Neurosci 7:62.
605 Franklin KBJ, Paxinos G (2007) The Mouse Brain in Stereotaxic Coordinates, Third Edition Edition. New
606 York, NY: Academic Press.

eNeuro Accepted Manuscript

607 Friedel RH, Plump A, Lu X, Spilker K, Jolicoeur C, Wong K, Venkatesh TR, Yaron A, Hynes M, Chen B,
608 Okada A, McConnell SK, Rayburn H, Tessier-Lavigne M (2005) Gene targeting using a
609 promoterless gene trap vector ("targeted trapping") is an efficient method to mutate a large
610 fraction of genes. Proc Natl Acad Sci U S A 102:13188-13193.
611 Grace AA, Floresco SB, Goto Y, Lodge DJ (2007) Regulation of firing of dopaminergic neurons and control
612 of goal-directed behaviors. Trends Neurosci 30:220-227.
613 Grant A, Manitt C, Flores C (2014) Haloperidol treatment downregulates DCC expression in the ventral
614 tegmental area. Neurosci Lett 575:58-62.
615 Grant A, Speed Z, Labelle-Dumais C, Flores C (2009) Post-pubertal emergence of a dopamine phenotype
616 in netrin-1 receptor-deficient mice. Eur J Neurosci 30:1318-1328.
617 Grant A, Hoops D, Labelle-Dumais C, Prevost M, Rajabi H, Kolb B, Stewart J, Arvanitogiannis A, Flores C
618 (2007) Netrin-1 receptor-deficient mice show enhanced mesocortical dopamine transmission
619 and blunted behavioural responses to amphetamine. Eur J Neurosci 26:3215-3228.
620 Hammond R, Blaess S, Abeliovich A (2009) Sonic hedgehog is a chemoattractant for midbrain
621 dopaminergic axons. PLoS One 4:e7007.
622 Hayes L, Ralls S, Wang H, Ahn S (2013) Duration of Shh signaling contributes to mDA neuron diversity.
623 Dev Biol 374:115-126.
624 Hayes L, Zhang Z, Albert P, Zervas M, Ahn S (2011) Timing of Sonic hedgehog and Gli1 expression
625 segregates midbrain dopamine neurons. J Comp Neurol 519:3001-3018.
626 Heussler HS, Suri M, Young ID, Muenke M (2002) Extreme variability of expression of a Sonic Hedgehog
627 mutation: attention difficulties and holoprosencephaly. Arch Dis Child 86:293-296.
628 Holm S (1979) A simple sequentially rejective multiple test procedure. Scand J Stat 6:65-70.
629 Hong M, Krauss RS (2013) Rescue of holoprosencephaly in fetal alcohol-exposed Cdon mutant mice by
630 reduced gene dosage of Ptch1. PLoS One 8:e79269.

eNeuro Accepted Manuscript

631 Hynes M, Porter JA, Chiang C, Chang D, Tessier-Lavigne M, Beachy PA, Rosenthal A (1995) Induction of
632 midbrain dopaminergic neurons by Sonic hedgehog. Neuron 15:35-44.
633 Jackson ME, Moghaddam B (2001) Amygdala regulation of nucleus accumbens dopamine output is
634 governed by the prefrontal cortex. J Neurosci 21:676-681.
635 Kabanova A, Pabst M, Lorkowski M, Braganza O, Boehlen A, Nikbakht N, Pothmann L, Vaswani AR,
636 Musgrove R, Di Monte DA, Sauvage M, Beck H, Blaess S (2015) Function and developmental
637 origin of a mesocortical inhibitory circuit. Nat Neurosci 18:872-882.
638 Koch M, Bubser M (1994) Deficient sensorimotor gating after 6-hydroxydopamine lesion of the rat
639 medial prefrontal cortex is reversed by haloperidol. Eur J Neurosci 6:1837-1845.
640 Kohl S, Heekeren K, Klosterkotter J, Kuhn J (2013) Prepulse inhibition in psychiatric disorders--apart from
641 schizophrenia. J Psychiatr Res 47:445-452.
642 Kwon YR, Jeong MH, Leem YE, Lee SJ, Kim HJ, Bae GU, Kang JS (2014) The Shh coreceptor Cdo is required
643 for differentiation of midbrain dopaminergic neurons. Stem Cell Res 13:262-274.
644 Lammel S, Hetzel A, Hackel O, Jones I, Liss B, Roeper J (2008) Unique properties of mesoprefrontal
645 neurons within a dual mesocorticolimbic dopamine system. Neuron 57:760-773.
646 Manitt C, Labelle-Dumais C, Eng C, Grant A, Mimee A, Stroh T, Flores C (2010) Peri-pubertal emergence
647 of UNC-5 homologue expression by dopamine neurons in rodents. PLoS One 5:e11463.
648 Manitt C, Mimee A, Eng C, Pokinko M, Stroh T, Cooper HM, Kolb B, Flores C (2011) The netrin receptor
649 DCC is required in the pubertal organization of mesocortical dopamine circuitry. J Neurosci
650 31:8381-8394.
651 Manitt C, Eng C, Pokinko M, Ryan RT, Torres-Berrio A, Lopez JP, Yogendran SV, Daubaras MJ, Grant A,
652 Schmidt ER, Tronche F, Krimpenfort P, Cooper HM, Pasterkamp RJ, Kolb B, Turecki G, Wong TP,
653 Nestler EJ, Giros B, Flores C (2013) dcc orchestrates the development of the prefrontal cortex
654 during adolescence and is altered in psychiatric patients. Transl Psychiatry 3:e338.

eNeuro Accepted Manuscript

655 Matise MP, Epstein DJ, Park HL, Platt KA, Joyner AL (1998) Gli2 is required for induction of floor plate
656 and adjacent cells, but not most ventral neurons in the mouse central nervous system.
657 Development 125:2759-2770.
658 Meyer U, Engler A, Weber L, Schedlowski M, Feldon J (2008) Preliminary evidence for a modulation of
659 fetal dopaminergic development by maternal immune activation during pregnancy.
660 Neuroscience 154:701-709.
661 Mille F, Tamayo-Orrego L, Levesque M, Remke M, Korshunov A, Cardin J, Bouchard N, Izzi L, Kool M,
662 Northcott PA, Taylor MD, Pfister SM, Charron F (2014) The Shh receptor Boc promotes
663 progression of early medulloblastoma to advanced tumors. Dev Cell 31:34-47.
664 Moghaddam B (2002) Stress activation of glutamate neurotransmission in the prefrontal cortex:
665 implications for dopamine-associated psychiatric disorders. Biol Psychiatry 51:775-787.
666 Okada A, Charron F, Morin S, Shin DS, Wong K, Fabre PJ, Tessier-Lavigne M, McConnell SK (2006) Boc is a
667 receptor for sonic hedgehog in the guidance of commissural axons. Nature 444:369-373.
668 Paxinos G, Franklin KBJ (2008) The Mouse Brain in Stereotaxic Coordinates, 3rd Edition. Amsterdam:
669 Elsevier/Academic Press.
670 Pierce RC, Kalivas PW (1997) A circuitry model of the expression of behavioral sensitization to
671 amphetamine-like psychostimulants. Brain Res Brain Res Rev 25:192-216.
672 Pokinko M, Moquin L, Torres-Berrio A, Gratton A, Flores C (2015) Resilience to amphetamine in mouse
673 models of netrin-1 haploinsufficiency: role of mesocortical dopamine. Psychopharmacology
674 (Berl) 232:3719-3729.
675 Reynolds LM, Makowski CS, Yogendran SV, Kiessling S, Cermakian N, Flores C (2015) Amphetamine in
676 adolescence disrupts the development of medial prefrontal cortex dopamine connectivity in a
677 DCC-dependent manner. Neuropsychopharmacology 40:1101-1112.
678 Roeper J (2013) Dissecting the diversity of midbrain dopamine neurons. Trends Neurosci 36:336-342.

eNeuro Accepted Manuscript

679 Scornaiencki R, Cantrup R, Rushlow WJ, Rajakumar N (2009) Prefrontal cortical D1 dopamine receptors
680 modulate subcortical D2 dopamine receptor-mediated stress responsiveness. Int J
681 Neuropsychopharmacol 12:1195-1208.
682 Seguela P, Watkins KC, Descarries L (1988) Ultrastructural features of dopamine axon terminals in the
683 anteromedial and the suprarhinal cortex of adult rat. Brain Res 442:11-22.
684 Stewart J, Badiani A (1993) Tolerance and sensitization to the behavioral effects of drugs. Behav
685 Pharmacol 4:289-312.
686 Swerdlow NR, Geyer MA (1998) Using an animal model of deficient sensorimotor gating to study the
687 pathophysiology and new treatments of schizophrenia. Schizophr Bull 24:285-301.
688 Swerdlow NR, Mansbach RS, Geyer MA, Pulvirenti L, Koob GF, Braff DL (1990) Amphetamine disruption
689 of prepulse inhibition of acoustic startle is reversed by depletion of mesolimbic dopamine.
690 Psychopharmacology (Berl) 100:413-416.
691 Tenn CC, Kapur S, Fletcher PJ (2005) Sensitization to amphetamine, but not phencyclidine, disrupts
692 prepulse inhibition and latent inhibition. Psychopharmacology (Berl) 180:366-376.
693 Van den Heuvel DM, Pasterkamp RJ (2008) Getting connected in the dopamine system. Prog Neurobiol
694 85:75-93.
695 Ventura R, Alcaro A, Cabib S, Conversi D, Mandolesi L, Puglisi-Allegra S (2004) Dopamine in the medial
696 prefrontal cortex controls genotype-dependent effects of amphetamine on mesoaccumbens
697 dopamine release and locomotion. Neuropsychopharmacology 29:72-80.
698 Vezina P (1993) Amphetamine injected into the ventral tegmental area sensitizes the nucleus
699 accumbens dopaminergic response to systemic amphetamine: an in vivo microdialysis study in
700 the rat. Brain Res 605:332-337.

eNeuro Accepted Manuscript

701 Vezina P, Blanc G, Glowinski J, Tassin JP (1991) Opposed Behavioural Outputs of Increased Dopamine
702 Transmission in Prefrontocortical and Subcortical Areas: A Role for the Cortical D-1 Dopamine
703 Receptor. Eur J Neurosci 3:1001-1007.
704 Vokes SA, Ji H, McCuine S, Tenzen T, Giles S, Zhong S, Longabaugh WJ, Davidson EH, Wong WH,
705 McMahon AP (2007) Genomic characterization of Gli-activator targets in sonic hedgehog-
706 mediated neural patterning. Development 134:1977-1989.
707 Volkow ND, Morales M (2015) The Brain on Drugs: From Reward to Addiction. Cell 162:712-725.
708 Wallen A, Perlmann T (2003) Transcriptional control of dopamine neuron development. Ann N Y Acad Sci
709 991:48-60.
710 Wang MZ, Jin P, Bumcrot DA, Marigo V, McMahon AP, Wang EA, Woolf T, Pang K (1995) Induction of
711 dopaminergic neuron phenotype in the midbrain by Sonic hedgehog protein. Nat Med 1:1184-
712 1188.
713 Watson RE, Jr., Wiegand SJ, Clough RW, Hoffman GE (1986) Use of cryoprotectant to maintain long-term
714 peptide immunoreactivity and tissue morphology. Peptides 7:155-159.
715 West MJ, Slomianka L, Gundersen HJ (1991) Unbiased stereological estimation of the total number of
716 neurons in thesubdivisions of the rat hippocampus using the optical fractionator. Anat Rec
717 231:482-497.
718 Yam PT, Charron F (2013) Signaling mechanisms of non-conventional axon guidance cues: the Shh, BMP
719 and Wnt morphogens. Curr Opin Neurobiol 23:965-973.
720 Yetnikoff L, Eng C, Benning S, Flores C (2010) Netrin-1 receptor in the ventral tegmental area is required
721 for sensitization to amphetamine. Eur J Neurosci 31:1292-1302.
722 Zhang W, Hong M, Bae GU, Kang JS, Krauss RS (2011) Boc modifies the holoprosencephaly spectrum of
723 Cdo mutant mice. Dis Model Mech 4:368-380.

724 Zhang W, Yi MJ, Chen X, Cole F, Krauss RS, Kang JS (2006) Cortical thinning and hydrocephalus in mice
725 lacking the immunoglobulin superfamily member CDO. Mol Cell Biol 26:3764-3772.

726

eNeuro Accepted Manuscript

eNeuro Accepted Manuscript

FIGURES LEGENDS

Figure 1. *Cdon* is expressed in proliferating progenitor cells of the ventral midbrain at E12.5

(A) Schematic illustration of a brain from e12.5 embryo showing the antero-posterior level used in the coronal sections shown in B-D. (B) *Cdon*$^{+/-}$ embryos exhibit staining for β-Gal(Cdon) expression in the ventral midbrain (middle panel), which is not seen in WT negative control (bottom panel). (C) Cdon immunolabeling appears throughout the dopamine progenitor zone in the ventral midbrain of a WT embryo (top and middle panels), while a control section stained without primary antibody (bottom panel) has no such labelling. (D) β-Gal(Cdon) expression relative to tyrosine hydroxylase (TH, a marker of mature dopamine neurons), Nuclear receptor related 1 (Nurr1, a marker of immature postmitotic dopamine neurons), and Ki67 (a marker of proliferation) indicates that Cdon overlaps mainly with the proliferative Ki67-positive zone.

Figure 2. The number of proliferating cells in the ventral midbrain of *Cdon*$^{-/-}$ embryos is increased at e12.5.

(A) Representative merged images of immunofluorescence for Ki67 (Green), TH (Red), and DAPI (Blue) in coronal slices of the ventral midbrain of embryos at e12.5. (B) Schematic illustrating the coronal plane of analysis. (C) The total number of Ki67 immunoreactive cells was significantly increased in *Cdon*$^{-/-}$ embryos relative to WT controls (Student's t-test, p=0.0069, Table 1-a), and (D) this effect was seen across the anterior-mid-posterior extent of the ventral midbrain ($ANOVA_{GenotypeXLevel}$, Main effect of Genotype, p=0.0003, Table 1-b). Whereas, (E) the total number of TH immunoreactive cells was similar between *Cdon*$^{-/-}$ embryos relative to WT

eNeuro Accepted Manuscript

controls (Student's t-test, p=0.498, Table 1-c), and (F) no genotype or level-based effect was observed at anterior, mid, or posterior levels of the ventral midbrain ($ANOVA_{GenotypeXLevel}$, Table 1-d). n=6-8 embryos/group.

Figure 3. Greater number of TH-positive neurons in the VTA of *Cdon*$^{-/-}$ mice at birth and in adulthood.

Total number of TH-positive neurons in the VTA (left, in red) and SN (right, in blue) in (A) postnatal day 0 (PND 0) and (B) adult mice as measured by stereology. A greater number of TH-positive neurons were observed in the VTA of *Cdon*$^{-/-}$ mice compared to WT controls at birth (Student's t-test, p<0.05, Table 1-e) and in adulthood (Student's t-test, p<0.01, Table 1-f). (C) Mouse brain atlas illustrations showing the VTA and SN sections that were included in this analysis, and representative TH-immunoreactivity in coronal sections of adult mice. n=4-5 mice/group. * p<0.05, ** p<0.01.

Figure 4. Greater dopamine and DOPAC concentrations in the mPFC, but not the NAcc or DS, of adult *Cdon*$^{-/-}$ mice.

(A) Brain samples were taken from each target region illustrated. (B) HPLC revealed a selective increase in the dopamine and DOPAC concentrations of the mPFC of *Cdon*$^{-/-}$ mice, an effect that was not seen in the NAcc or DS (Table 1-g). n=7-10 animals/group. * = p<0.05, ** = p<0.01

eNeuro Accepted Manuscript

768 **Figure 5. Increased number of dopamine varicosities in the mPFC of *Cdon*$^{-/-}$ mice.**

769 Stereological quantifications of the number of dopamine varicosities in (A) the cingulate (Cg),
770 the prelimbic (PL), and the infralimbic (IL) pregenual mPFC. (B) The total number of dopamine
771 varicosities was greater in the *Cdon*$^{-/-}$ mice compared to WT controls ($ANOVA_{Genotype}$, p=0.0079,
772 Table 1-h). (C) There were no differences in the volume that dopamine varicosities occupied in
773 the mPFC between *Cdon*$^{-/-}$ and WT mice (Table 1-i). Likewise, (D) an increase in the density of
774 dopamine varicosities was observed in all three subregions ($ANOVA_{Genotype}$, p=0.0073, Table 1-j).
775 (E) Representative photomicrographs at high magnification illustrating differences in the total
776 number/density of dopamine varicosities in the PL mPFC comparing *Cdon*$^{-/-}$ and WT mice. n=3
777 mice/group.

778

779 **Figure 6. Locomotor activity testing of *Cdon*$^{-/-}$ mice reveals attenuation of behavioral plasticity**
780 **in adulthood.**
781 (A) First exposure/habituation to the locomotor testing environment, (B) habituation to
782 handling and saline injection (injection denoted by "S" vertical line), and (C) first injection of
783 amphetamine (injection denoted by "A" vertical line, 2.5mg/kg i.p.) all produce
784 indistinguishable levels of locomotor activity between *Cdon*$^{-/-}$ and WT controls (Table 1-k, Table
785 1-l, Table 1-m, respectively). In contrast, (D) a sensitizing schedule of amphetamine injections
786 (E) induced robust locomotor sensitization in WT controls, while locomotor sensitization in
787 *Cdon*$^{-/-}$ mice was greatly attenuated ($ANOVA_{GenotypeXTime}$, p=0.043, Table 1-n). (F) Stereotypy
788 counts were increased in WT controls, but did not change significantly in *Cdon*$^{-/-}$ mice. n=6-10
789 animals/group.

eNeuro Accepted Manuscript

Figure 7. Sensorimotor gating function is attenuated in adult *Cdon*$^{-/-}$ mice.

Pre-pulse inhibition (PPI) is measured relative to the baseline startle for each mouse and is shown according to the volume of each pre-pulse (pp3, pp5, pp7, pp10, pp15, pp20), which is the number of dB above environmental white noise (70dB). The PPI% percentage was calculated for each pre-pulse volume (mean pre-pulse) as a percentage of the un-signaled startle intensity (mean startle) for each individual mouse, and the baseline movement in the absence of acoustic pulses (mean null) was subtracted from all values: PPI% = 1-(mean pre-pulse – mean null)/(mean startle – mean null)*100. When the normalized PPI for each individual were compared by 2-way ANOVA (pp volume x Genotype) significant effects of volume ($ANOVA_{pp\ volume}$, $p<0.0001$, Table 1-p) and genotype ($ANOVA_{Genotype}$, $p<0.001$, Table 1-p) were observed on PPI.

eNeuro Accepted Manuscript

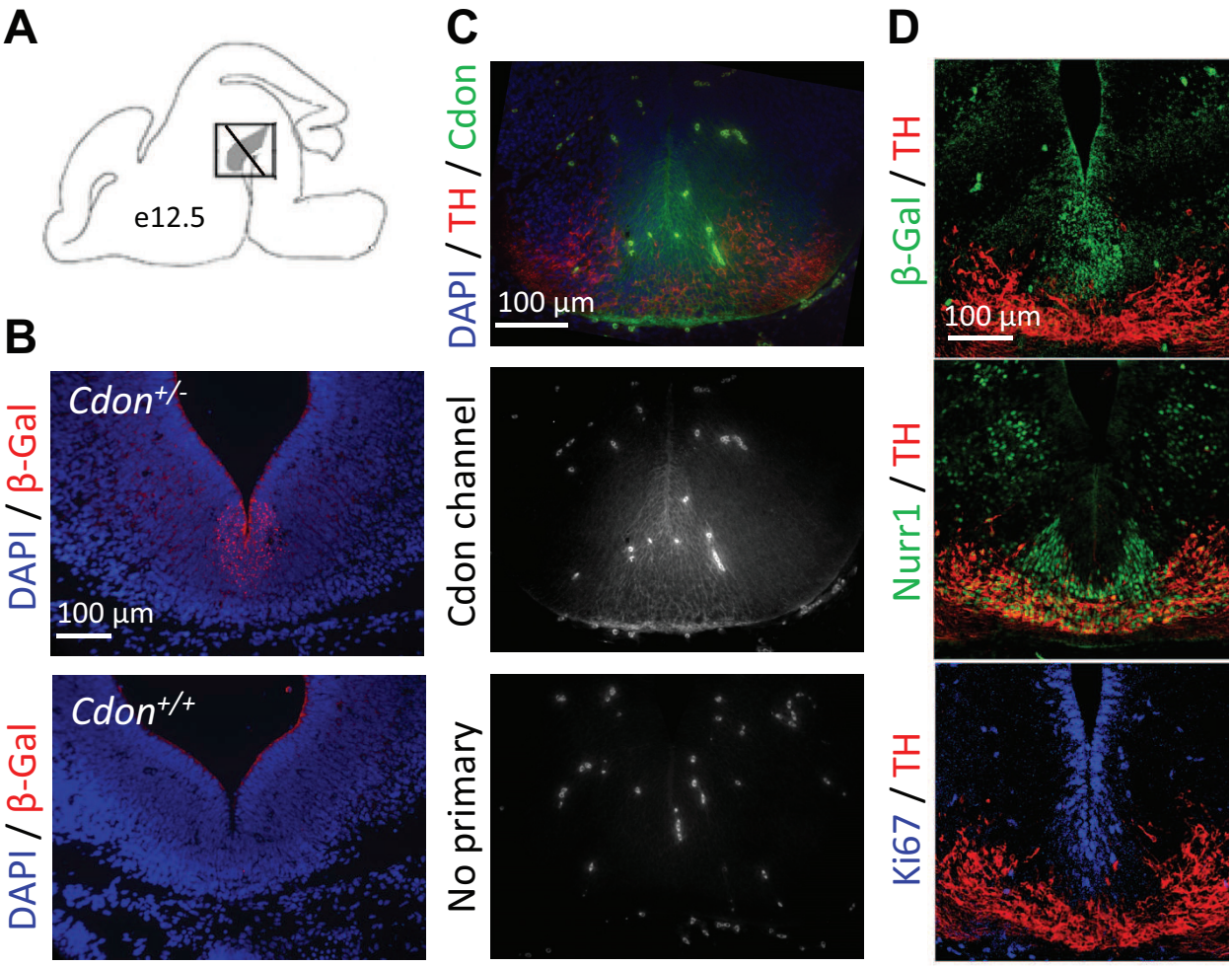

eNeuro Accepted Manuscript

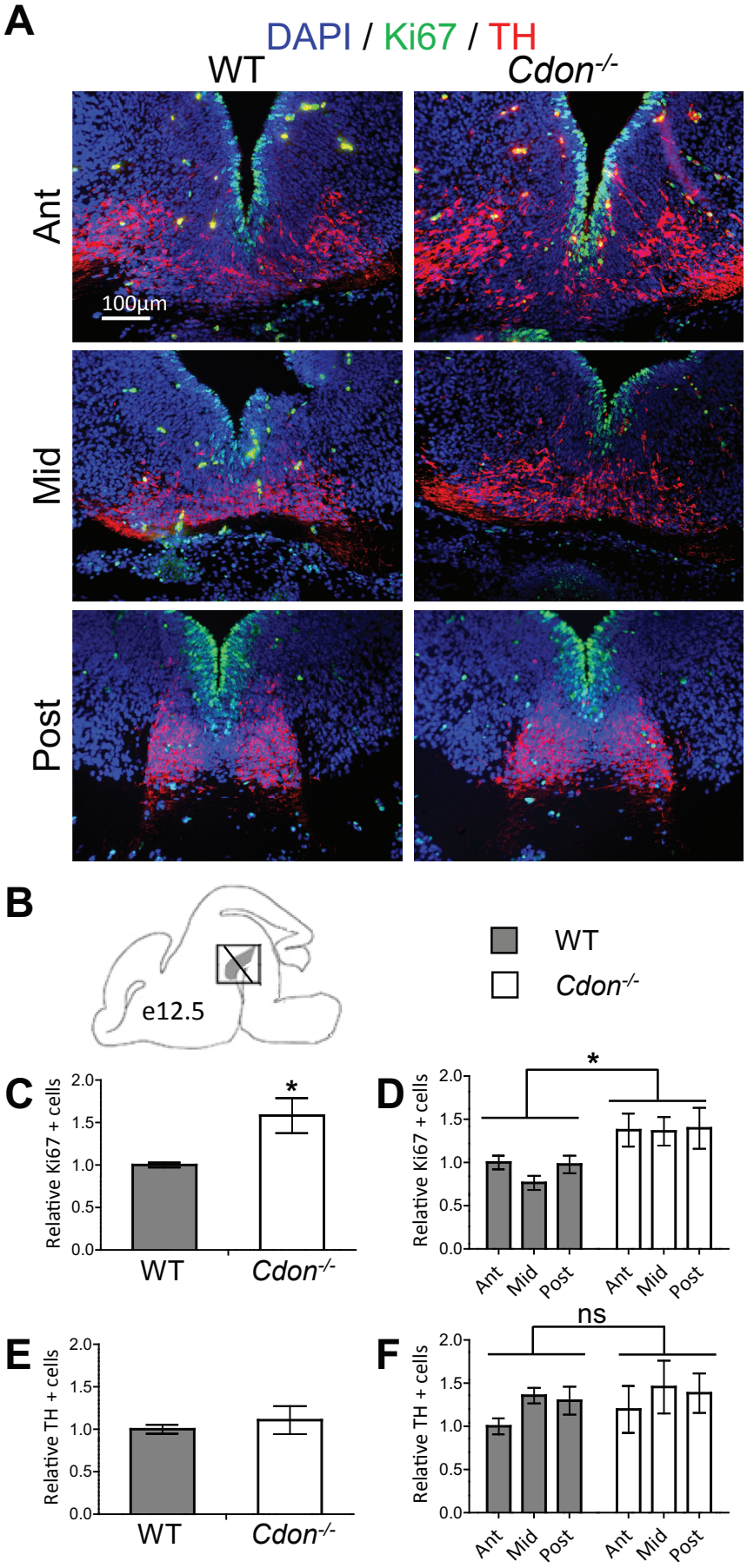

eNeuro Accepted Manuscript

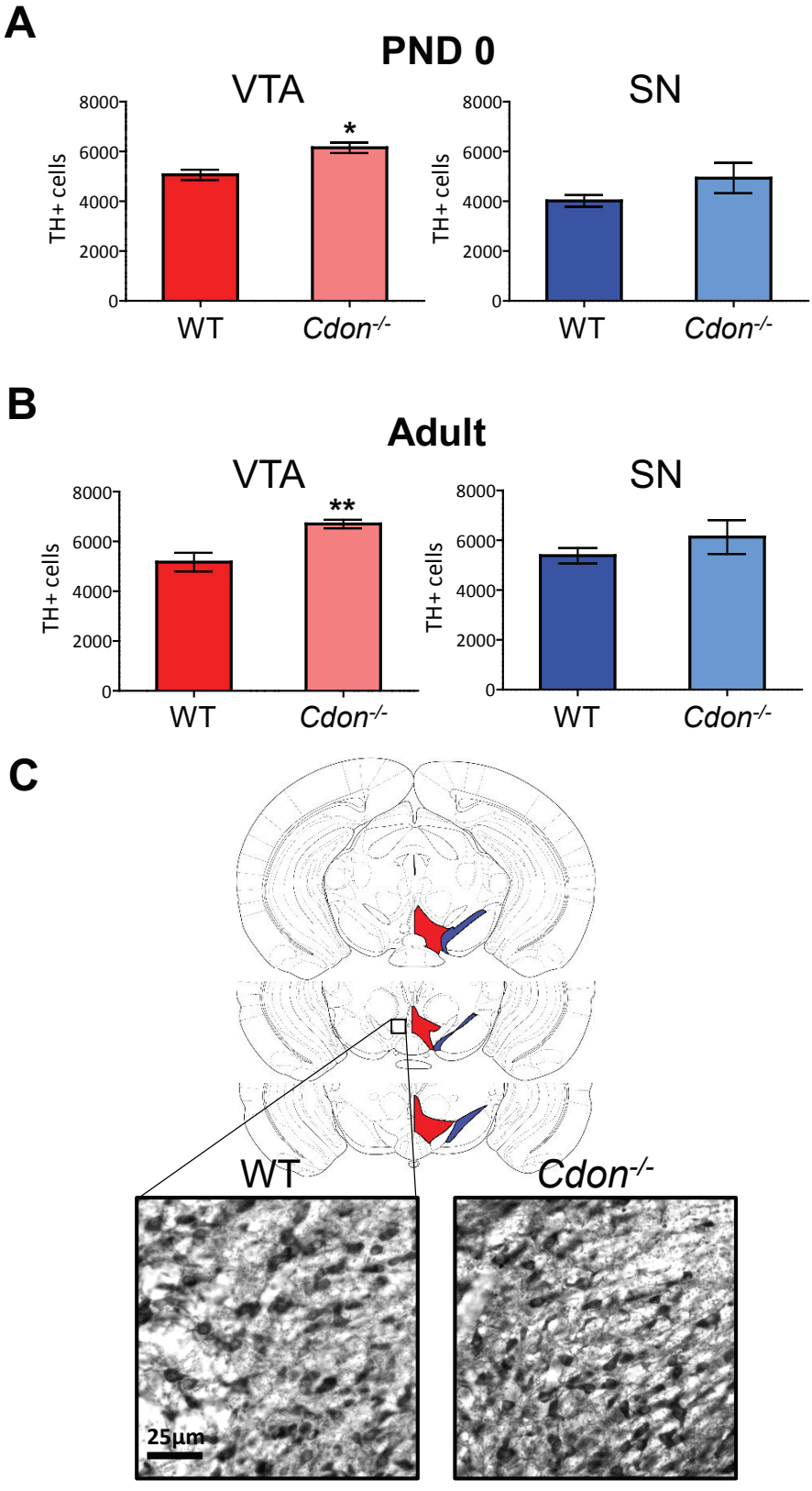

eNeuro Accepted Manuscript

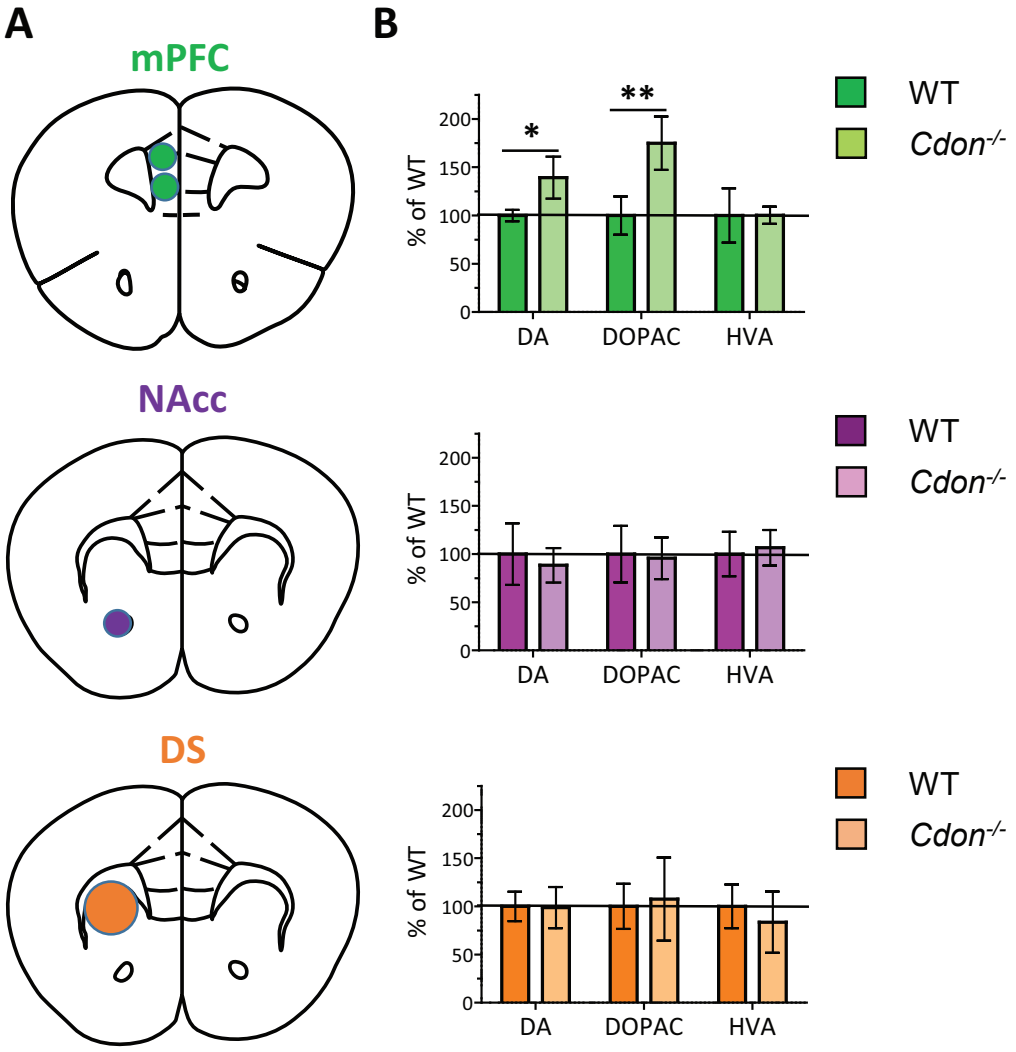

eNeuro Accepted Manuscript

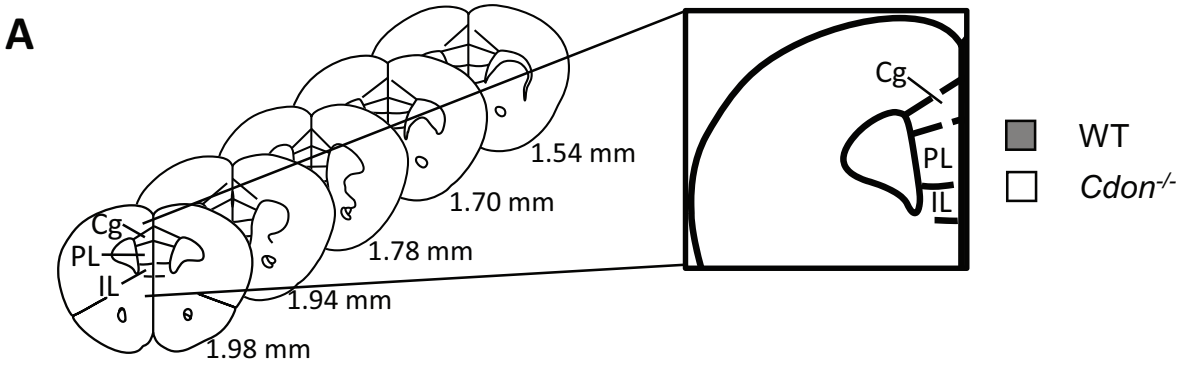

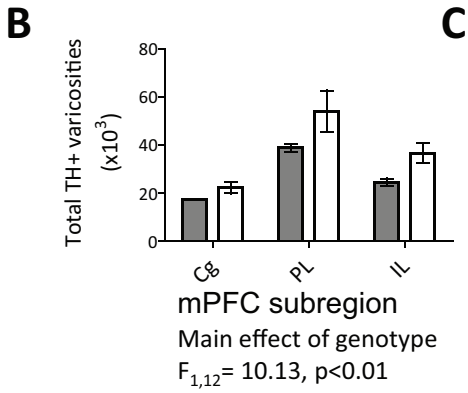

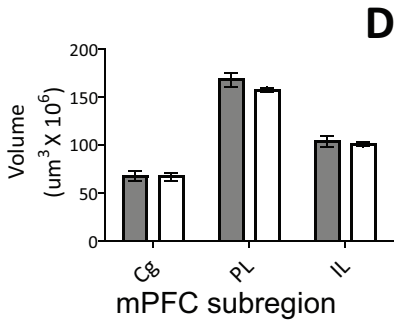

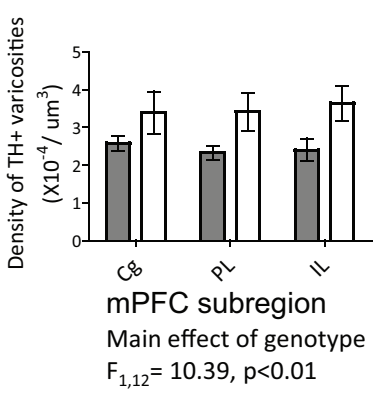

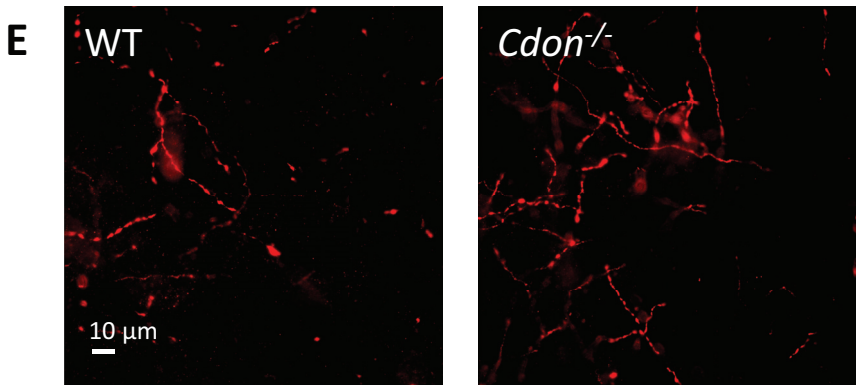

eNeuro Accepted Manuscript

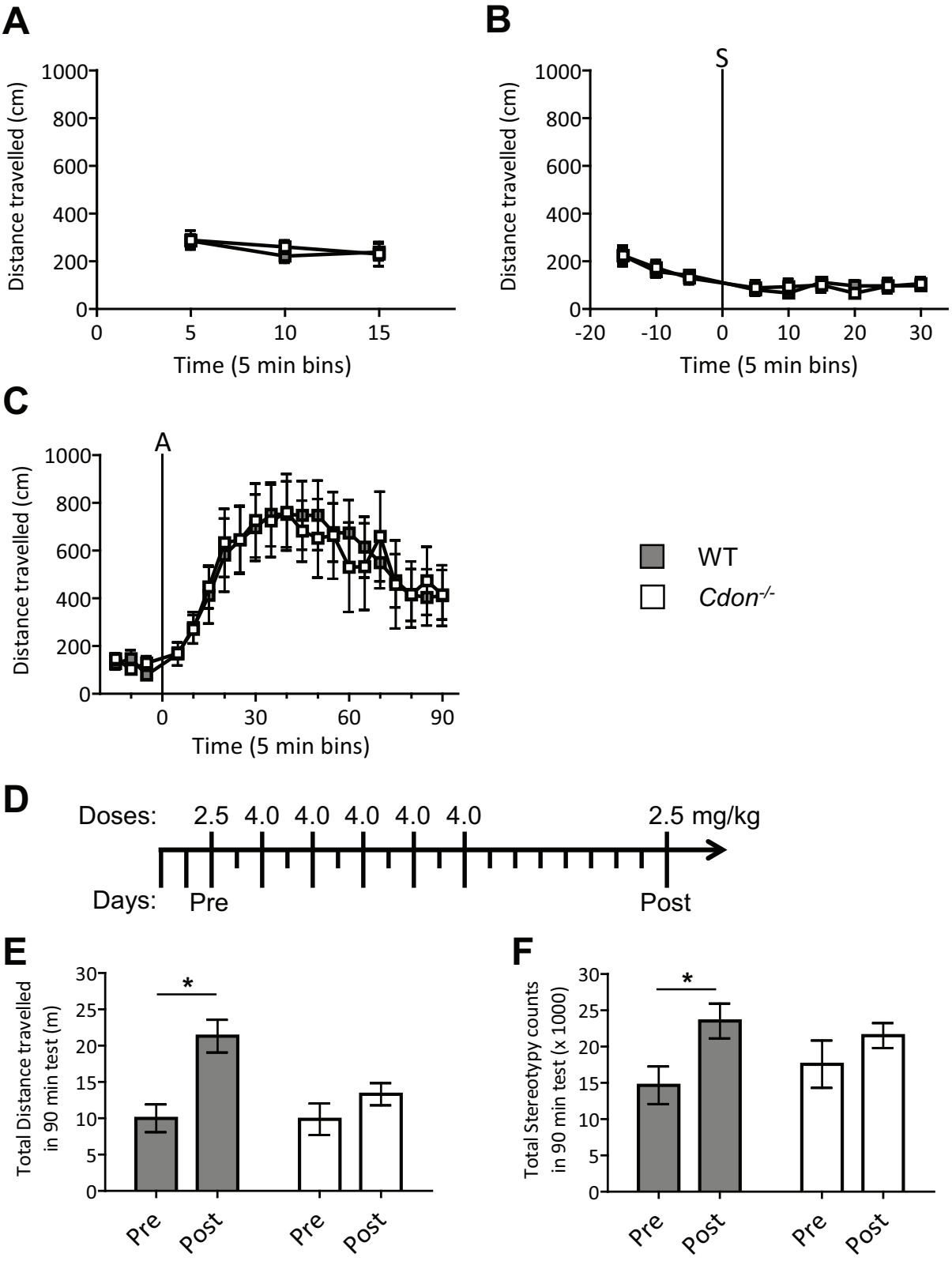

eNeuro Accepted Manuscript

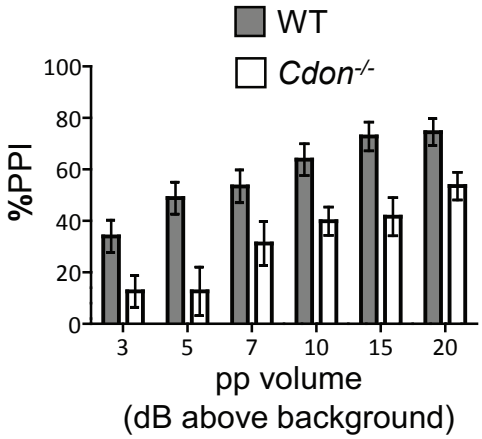

Main effect of genotype
$F_{1,295}$= 13.12, p= 0.0006

eNeuro Accepted Manuscript

Table 1. Statistical tests and values

Graph	Type of Test	Statistical Values
a. Figure 2C	Unpaired t-test (two-tailed)	t_{12}= 3.252, p= 0.0069 *
b. Figure 2D	ANOVA (Genotype X Level)	$F_{2,34}$= 0.3468, p= 0.7094
	ANOVA (Genotype)	$F_{1,34}$= 15.96, p= 0.0003 *
	ANOVA (Level)	$F_{2,34}$= 0.5282, p= 0.5944
c. Figure 2E	Unpaired t-test (two-tailed)	t_{12}= 0.6990, p= 0.4979
d. Figure 2F	ANOVA (Genotype X Level)	$F_{2,34}$= 0.04603, p= 0.9551
	ANOVA (Genotype)	$F_{1,34}$= 0.6569, p= 0.4233
	ANOVA (Level)	$F_{2,34}$= 1.357, p= 0.2711
e. Figure 3A (VTA)	Unpaired t-test (two-tailed)	t_{6}= 3.655, p= 0.0105 *
Figure 3A (SN)	Unpaired t-test (two-tailed)	t_{6}= 1.399, p= 0.2114
f. Figure 3B (VTA)	Unpaired t-test (two-tailed)	t_{8}= 3.747, p= 0.0056 *
Figure 3B (SN)	Unpaired t-test (two-tailed)	t_{8}= 1.004, p= 0.3448
g. Figure 4B (mPFC)	DA Unpaired t-test (two-tailed)	t_{15}= 5.482, p<0.0001 *
	DOPAC Unpaired t-test (two-tailed)	t_{15}= 6.529, p<0.0001 *
	HVA Unpaired t-test (two-tailed)	t_{15}= 0.02491, p= 0.9805
Figure 4B (NAcc)	DA Unpaired t-test (two-tailed)	t_{15}= 0.8655, p= 0.4004
	DOPAC Unpaired t-test (two-tailed)	t_{15}= 0.3288, p= 0.7469
	HVA Unpaired t-test (two-tailed)	t_{15}= 0.6184, p= 0.5456
Figure 4C (DS)	DA Unpaired t-test (two-tailed)	t_{15}= 0.1534, p= 0.8801
	DOPAC Unpaired t-test (two-tailed)	t_{15}= 0.4683, p= 0.6463
	HVA Unpaired t-test (two-tailed)	t_{15}= 1.245, p= 0.2321
h. Figure 5B	ANOVA (Genotype X subregion)	$F_{2,12}$= 0.8166, p= 0.465
	ANOVA (Genotype)	$F_{1,12}$= 10.13, p= 0.0079 *
	ANOVA (Subregion)	$F_{2,12}$= 21.25, p= 0.0001 *
i. Figure 5C	ANOVA (Genotype X subregion)	$F_{2,12}$= 0.5533, p= 0.5891
	ANOVA (Genotype)	$F_{1,12}$= 1.431, p= 0.2547
	ANOVA (Subregion)	$F_{2,12}$= 205.6, p<0.0001 *
j. Figure 5D	ANOVA (Genotype X subregion)	$F_{2,12}$= 0.1561, p= 0.8572
	ANOVA (Genotype)	$F_{1,12}$= 10.39, p= 0.0073 *
	ANOVA (Subregion)	$F_{2,12}$= 0.07934, p= 0.9242
k. Figure 6A	ANOVA (Genotype X Time)	$F_{2,30}$= 0.6911, p= 0.5088
	ANOVA (Genotype)	$F_{1,30}$= 0.06015, p= 0.8096
	ANOVA (Time)	$F_{2,30}$= 4.016, p= 0.0285 *
l. Figure 6B	ANOVA (Genotype X Time)	$F_{2,120}$= 0.2720, p= 0.9739
	ANOVA (Genotype)	$F_{1,120}$= 0.0003935, p= 0.9844
	ANOVA (Time)	$F_{8,120}$= 83615, p<0.0001 *
m. Figure 6C	ANOVA (Genotype X Time)	$F_{20,300}$= 0.2543, p= 0.9996
	ANOVA (Genotype)	$F_{1,300}$= 0.001303, p= 0.9717
	ANOVA (Time)	$F_{20,300}$= 14.34, p<0.0001 *
n. Figure 6E	ANOVA (Genotype X Test)	$F_{1,15}$= 4.882, p= 0.0431 *
	ANOVA (Genotype)	$F_{1,15}$= 2.417, p= 0.1409
	ANOVA (Test)	$F_{1,15}$= 17.18, p= 0.0009 *
o. Figure 6F	ANOVA (Genotype X Test)	$F_{1,14}$= 0.9707, p= 0.3412
	ANOVA (Genotype)	$F_{1,14}$= 0.02339, p= 0.8806
	ANOVA (Test)	$F_{1,14}$= 6.592, p= 0.0223 *
p. Figure 7	ANOVA (Genotype X pp volume)	$F_{5,295}$= 0.9344, p= 0.4589
	ANOVA (Genotype)	$F_{1,295}$= 13.12, p= 0.0006 *
	ANOVA (pp volume)	$F_{5,295}$= 23.5, p<0.0001 *